Heliyon 10 (2024) e32139

Contents lists available at ScienceDirect

Heliyon

journal homepage: www.cell.com/heliyon

Research article

APOBEC3-related mutations in the spike protein-encoding region facilitate SARS-CoV-2 evolution

Jiaying Shen [a,b,c,1], Xinxin Xu [e,1], Junyan Fan [b,c,d,1], Hongsen Chen [b,c,d,1], Yue Zhao [b,c,d], Weijin Huang [f], Wenbin Liu [b,c,d], Zihan Zhang [a,b,c], Qianqian Cui [f], Qianqian Li [f], Zheyun Niu [a,b,c], Dongming Jiang [a,b,c], Guangwen Cao [a,b,c,d,*]

[a] *Tongji University School of Medicine, Tongji University, Shanghai 200120, China*
[b] *Key Laboratory of Biological Defense, Ministry of Education, China*
[c] *Shanghai Key Laboratory of Medical Bioprotection, China*
[d] *Department of Epidemiology, Second Military Medical University, Shanghai, China*
[e] *Department of Gynecology, Shanghai First Maternity and Infant Hospital, School of Medicine, Tongji University, Shanghai, 200092, China*
[f] *Institute for Biological Product Control, National Institutes for Food and Drug Control (NIFDC), WHO Collaborating Center for Standardization and Evaluation of Biologicals, NHC Key Laboratory of Research on Quality and Standardization of Biotech Products and NMPA Key Laboratory for Quality Research and Evaluation of Biological Products, 102629 Beijing, China*

ARTICLE INFO

Keywords:
COVID-19
SARS-CoV-2
APOBEC3
A3B
RNA editing
Inflammation

ABSTRACT

SARS-CoV-2 evolves gradually to cause COVID-19 epidemic. One of driving forces of SARS-CoV-2 evolution might be activation of apolipoprotein B mRNA editing catalytic subunit-like protein 3 (APOBEC3) by inflammatory factors. Here, we aimed to elucidate the effect of the APOBEC3-related viral mutations on the infectivity and immune evasion of SARS-CoV-2. The APOBEC3-related C > U mutations ranked as the second most common mutation types in the SARS-CoV-2 genome. mRNA expression of *APOBEC3A* (*A3A*), *APOBEC3B* (*A3B*), and *APOBEC3G* (*A3G*) in peripheral blood cells increased with disease severity. *A3B*, a critical member of the APOBEC3 family, was significantly upregulated in both severe and moderate COVID-19 patients and positively associated with neutrophil proportion and COVID-19 severity. We identified USP18 protein, a key molecule centralizing the protein-protein interaction network of key APOBEC3 proteins. Furthermore, mRNA expression of *USP18* was significantly correlated to *ACE2* and *TMPRSS2* expression in the tissue of upper airways. Knockdown of *USP1*8 mRNA significantly decreased *A3B* expression. Ectopic expression of *A3B* gene increased SARS-CoV-2 infectivity. C > U mutations at S371F, S373L, and S375F significantly conferred with the immune escape of SARS-CoV-2. Thus, APOBEC3, whose expression are upregulated by inflammatory factors, might promote SARS-CoV-2 evolution and spread via upregulating USP18 level and facilitating the immune escape. A3B and USP18 might be therapeutic targets for interfering with SARS-CoV-2 evolution.

1. Introduction

The coronavirus disease 2019 (COVID-19) pandemic, caused by severe acute respiratory syndrome coronavirus 2 (SARS-CoV-2)

* Corresponding author. Department of Epidemiology, Second Military Medical University, Shanghai, China.
E-mail address: gcao@smmu.edu.cn (G. Cao).
[1] These authors have contributed equally to this article.

https://doi.org/10.1016/j.heliyon.2024.e32139
Received 10 December 2023; Received in revised form 28 May 2024; Accepted 29 May 2024
Available online 29 May 2024

(reviewed in) [1], has a profound impact on public health and economy [2]. SARS-CoV-2 is an enveloped, single-stranded positive-sense RNA virus with RNA-dependent RNA polymerase (reviewed in) [3,4], which helps rectify replication errors [5]. Genomic sequencing has revealed numerous novel mutation sites in the SARS-CoV-2 genome [6–10]. Understanding the SARS-CoV-2 evolution is crucial for tracking its global transmission and developing timely prophylactic options.

Apolipoprotein B mRNA editing catalytic subunit-like proteins (APOBECs), the zinc-dependent deaminase family, have an important impact on viral suppression and evolution [11]. They edit viral genome by recognizing specific nucleotides, compared to random genetic mutations [12,13]. APOBECs comprise 11 genes, namely *APOBEC1* (*A1*), *APOBEC2* (*A2*), *APOBEC3A* (*A3A*), *APOBEC3B* (*A3B*), *APOBEC3C* (*A3C*), *APOBEC3D* (*A3D*), *APOBEC3F* (*A3F*), *APOBEC3G* (*A3G*) and *APOBEC3H* (*A3H*), *APOBEC4* (*A4*) and activation-induced cytidine deaminase (*AICDA*) (reviewed in) [14]. Interferon (IFN) can increase the expression of APOBEC3 by which may cause viral suppression [15]. The APOBEC-induced mutagenesis contributes to the formation of variants with increased drug resistance and immune escape capacity (reviewed in) [16]. A1 [17], A3A [18,19], A3B [20] and A3G enzymes [21] target certain cellular single-stranded RNA for C > U editing. Besides, *A4* gene has been reported to be highly expressed in cell parts targeted by SARS-CoV-2 [22], which may be associated with viral replication. Notably, the APOBEC3-related C > U mutation accounts for 52 % of all non-synonymous single mutations in the SARS-CoV-2 genome [23]. A3A enzyme is also an important host factor that promotes mutations in the SARS-CoV-2 genome [24]. Other experimental evidence shows that A3A, A1 and A3G proteins can edit specific sites of viral RNA to produce C > U mutations [25], implying an important role of APOBEC proteins in viral evolution.

In the present study, we aimed to provide new insights into the impact of APOBEC3-mediated C > U mutations on the infectivity and immune evasion of SARS-CoV-2, which have not been well documented. We identified the correlation of APOBEC3 between immune cells and key genes related to virus invasion in COVID-19 patients to clarify its role in viral infection. Subsequently, we identified key mutated sites in the RBD (receptor binding domain) region of SARS-CoV-2 which facilitates immune escape.

2. Methods and materials

1 Data Collection

Datasets GSE157103 and GSE162562 from the Gene Expression Omnibus (GEO) database (https://www.ncbi.nlm.nih.gov/geo/GEO) were downloaded and combined to obtain the expression of APOBECs profile in peripheral blood mononuclear cells (PBMCs) of COVID-19 patients with different disease statuses and in healthy controls. RNA-sequencing (RNA-seq) data of PBMCs samples were analyzed from GSE157103 consisting of 128 COVID-19 and non-COVID-19 patients with various disease severity, and GSE162562 consisting of 43 asymptomatic subjects seropositive for SARS-CoV-2, 52 seronegative subjects who were highly exposed to SARS-CoV-2, 4 COVID-19 patients with mild symptoms and 5 healthy controls. Additionally, the GSE156063 and GSE157103 datasets were downloaded to obtain mRNA expression data of *ACE2*, *TMPRSS2*, and ubiquitin-specific protease 18 (*USP18*). GSE156063 contained RNA-sequencing data of upper airway samples from 234 patients infected with SARS-CoV-2.

SARS-CoV-2 sequences were obtained from the GISAID database (https://www.gisaid.org/), which were collected from the first appearance of COVID-19 to the May 1, 2021. We used the Wuhan-Hu-1 strain (GenBank: MN908947.3) as a reference sequence. Utilizing Python 3.7.4 software, MAFFT, and the mutation annotation tool snpEFF, we conducted sequence alignment and annotated genomic structural data. To carry out sequence phylogenetic analysis, Clustal W was employed for multiple sequence alignment. Maximum Likelihood Estimate was then used to construct the phylogenetic tree, which was subsequently visualized with ITOL. The PyMOL software was used to predict the effects of point mutations on the crystal structure change of the RBD region of the spike protein and its interactions with angiotensin-converting enzyme 2 (ACE2).

2 Data analysis

We investigated the differential expression of genes (DEGs) in 100 PBMC samples obtained from patients with different disease severity. The median values of A3A, A3B, and A3G genes were used as references for analysis, respectively. $|\log FC \text{ (fold change)}| > 1$ and $P < 0.05$ were utilized as filter conditions to analyze the related DEGs via the DESeq2 R package. We used the CIBERSORT algorithm [26] to assess the correlation between the expression levels of *A3A*, *A3B*, and *A3G* genes and the proportion of each immune cell type in individuals infected with SARS-CoV-2 with different disease severity. Additionally, we analyzed the correlation between the expression of *USP18* gene and the expression of *ACE2* or *TMPRSS2* gene in the upper airway samples from GSE156063 and in the PBMCs samples from GSE157103, respectively. To construct protein-protein interaction (PPI) networks, the STRING database (https://cn.string-db.org/) [27] was used to integrate and score the associations of top 10 up-regulated proteins with A3A, A3B and A3G proteins, whose data were derived from the mining of literatures, databases of interaction experiments, and computational interaction predictions based on genomic context analysis. Other R packages like org.Hs.eg.db, clusterProfiler, enrichplot, pheatmap, ggplot2 and VennDiagram were also used to complete GO and KEGG analysis, expression profiles related to *A3A*, *A3B* and *A3G* genes, and images making.

3 Cell Culture

Human liver cancer cell Huh7, human cervical cancer cell HeLa, renal cell HEK293T, and non-small cell lung cancer cell NCI–H1650 (H1650) were obtained from the cell bank of the Chinese Academy of Sciences Shanghai Branch (Shanghai, China). The cell lines were cultured in Dulbecco's modified Eagle's medium (DMEM) supplemented with 10 % fetal bovine serum (FBS) and 1 %

penicillin (100 IU/ml) -streptomycin (100 μg/mL) at 37 °C in 5 % CO_2. H1650 and Huh7 were chosen as they could be infected by SARS-CoV-2 [28], while HEK293T and HeLa were transfected with its receptor ACE2 via a lentivirus package system, to enhance their susceptibility to viral infection.

4 Plasmid Construction and Preparedness

Plasmids encoding A3B and ACE2 protein were synthesized by the Hunan Fenghui Biotechnology Company (Hunan, China) and the Haijihaoge Biotechnology Company (Shanghai, China), respectively. Plasmids pHAGE-CMV-Luc2-IRES-ZsGreen-W, pTwist-SARS-CoV-2Δ18, and pTwist-SARS-CoV-2Δ18 D614G were purchased from the Addgene (Teddington, UK), with the item numbers of 164,432, 164,436, and 164,437, respectively. A single-point mutation was created in the RBD region of the pTwist-SARS-CoV-2Δ18 D614G plasmid according to APOBEC3-targeted TCW (W = A or T) motif, as the RBD region can greatly impact the virus's capacity to infect cells and evade neutralizing antibodies [29]. We extracted plasmids using the Plasmid Extraction Kit (QIAGEN 12963, Dusseldorf, Germany).

5 Construction of ACE2-overexpressing cells

HEK293T cells were co-transfected with an ACE2-expressing plasmid, psPAX2 (Addgene 12,260, Teddington, UK) and pMD2.G (Addgene 12,259, Teddington, UK) to generate lentivirus using Lipofectamine™ 3000 transfection reagent (Invitrogen L3000075, Waltham, MA) according to the manufacturer's instructions. The harvested supernatant was filtered through a 0.45 μm filter and subsequently utilized as lentivirus for transduction. HEK293T and HeLa were seeded in a 6-well plate, respectively, and the lentivirus was added using culture medium without antibiotics, along with 5 μg/ml of Polybrene (Absin abs42025397, Shanghai, China). After an incubation of 8 h (h), the medium was replaced with fresh medium, and puromycin (Invivogene ant-pr-1, Hong Kong, China) was used to select the target cells in the following 2 weeks. Real-time quantitative PCR (RT-qPCR) was conducted to validate mRNA expression of *ACE2* in the target cells.

6 RNA Extraction, RT-qPCR, and Western Blot

Total RNA was isolated using TRIzol (Invitrogen 15596026, Waltham, MA) method and reversely transcribed into cDNA using the Reverse-Transcript Kit (TAKARA RR820A, Shiga, Japan). RT-qPCR was performed using the TB GreenTM Premix Ex Taq TM Kit (TAKARA). The primers are listed in Supplementary Table 1. The data of RT-qPCR were analyzed by the comparative cycle threshold (CT) method and *GAPDH* gene served as a reference. Western blot analysis was performed as previously described [30]. The antibodies against A3B protein (Abcam ab184990, Cambridge, UK) and β-actin (Abcam ab184990, Boston, MA) were used. β-actin served as a loading marker.

7 Small Interfering RNA Interference Assay

Small-interfering RNAs (siRNAs) were chemically synthesized by the Ruibo Biotech Company (Shanghai, China). siRNAs were transfected into target cells using Lipofectamine™ RNAiMAX Transfection Reagent (Invitrogen 13,778-50, Waltham, MA). The transfection effects were analyzed by RT-qPCR and Western blot analyses.

8 Generation, Infection and Neutralization Assay of SARS-CoV-2 Pseudovirus

Pseudovirus carrying SARS-CoV-2 spike gene was produced using a vesicular stomatitis virus (VSV) pseudovirus package system [31]. The seeding density of HEK-293T cells was optimized to 5–7 $\times$ 10^5 cells/mL before transfection. Subsequently, cells with 70%–90 % confluence were infected with 15 mL of VSV-ΔG-G* pseudovirus. At the same time, the cells were transfected with 30 μg of the spike (S) protein-expressing plasmid with Lipofectamine™ 3000. After 6–8 h, the medium was replaced. The supernatant was collected after 24h' incubation. Wild-type SARS-CoV-2 S pseudovirus and Omicron BA.4/5 S protein pseudovirus were constructed, respectively, as previously reported [31]. To assess the pseudovirus infectivity, Huh7 cells were seeded in 96-well plates, exposed to 50 μL of target pseudoviruses mixed with 50 μL of medium, and then harvested between the 36th and 48th h following the transfection. Luciferase activity was measured and normalized using the reference sequence set as 1. The pseudovirus neutralization assay was performed as described in the previous literature [32]. Neutralizing monoclonal antibody to the SARS-CoV-2 spike (Catalog#40591-MM43) was purchased from Yiqiao Shenzhou Company (Beijing, China). Before infection, Huh7 cells were seeded in 96-well plates with a density of 1.5–2 $\times$ 10^4 cells/mL. After serially diluted, 55 μL of antibody was added into each well containing 55 μL of pseudovirus. After 1 h incubation at room temperature, mixture was added to cells in each well. Luciferase reporter assay was performed to detect the relevant signal at the 48th and 72nd h. The neutralization ability was measured by 50 % inhibitory dilution (EC_{50}) and normalized using the reference with a baseline value of 1.

9 Luciferase Reporter Assay

Cells were seeded in 96-well plates at a density of 1.5–2 $\times$ 10^4 cells per well in triplicate, and pseudovirus was added to each well. After the medium was replaced with passive lysis solution, the 96-well plates were vortexed adequately at room temperature.

Subsequently, cell lysate and 50 μL of Luciferase Assay Reagent II were added sequentially to each well, and the reporter gene expression was detected using a microplate reader (Biotek, Agilent, CA).

10 Statistical Analysis

Statistical analysis was performed using R software. The experimental data were presented as mean values ± standard deviation ($\bar{x} \pm S$). The continuous variables and categorical variables were compared using the Student's *t*-test and Chi-square test, respectively [33]. One-way analysis of variance (ANOVA) was employed to compare three samples or more. Non-parametric tests were used for data that did not meet the criteria for normal distribution or homogeneity. A statistically significant difference was defined as $P < 0.05$.

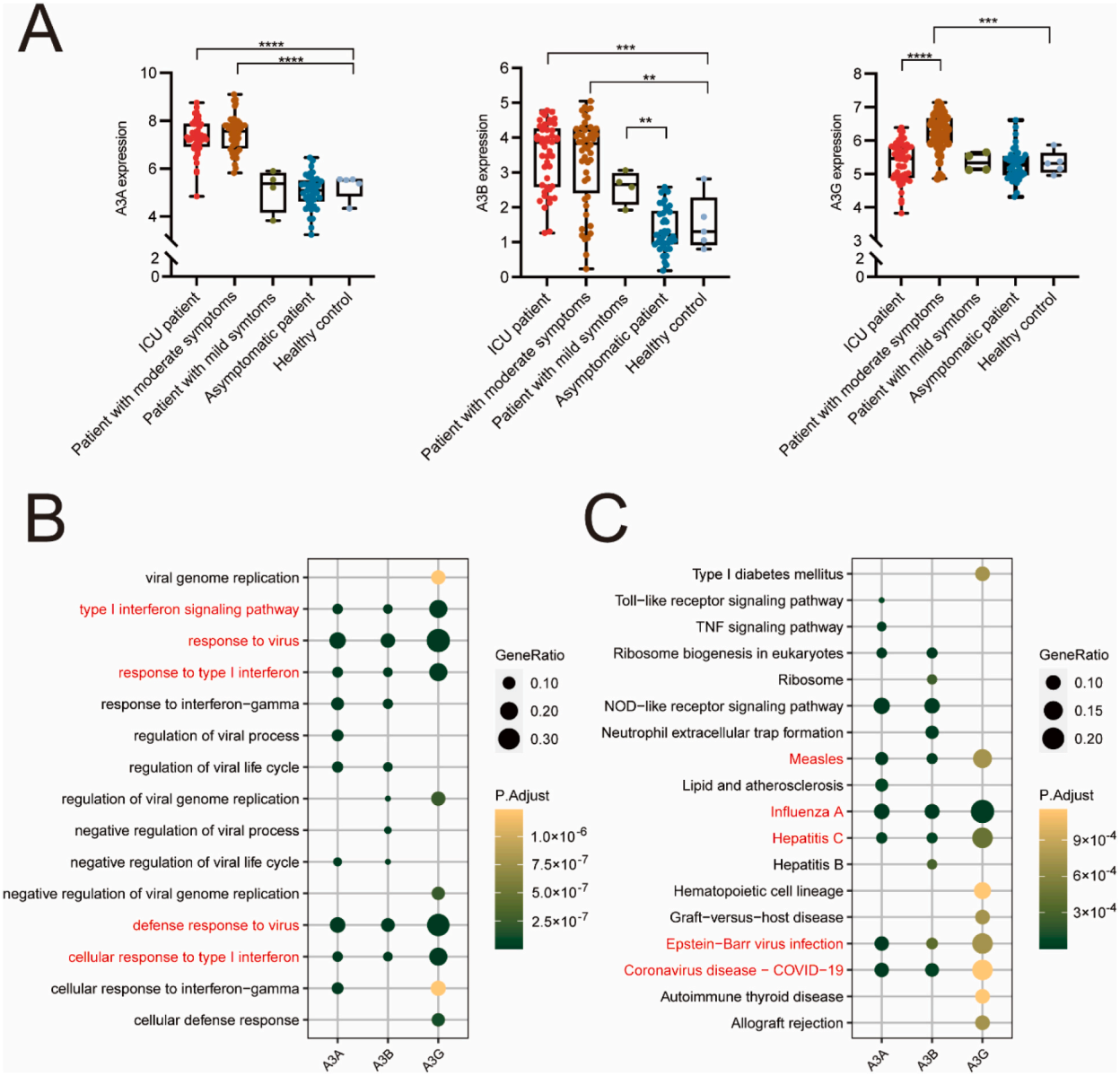

Fig. 1. Expression patterns of APOBEC3 members A3A, A3B, and A3G and their associated gene functions and signaling pathways in PBMCs of subjects with or without SARS-CoV-2 infection (A) Expression of *A3A* (left), *A3B* (middle), and *A3G* (right) genes in PBMCs of subjects with or without SARS-CoV-2 infection. (B) GO analysis of gene functions of *A3A*, *A3B*, and *A3G*-related genes. (C) KEGG analysis of signaling pathways of *A3A*, *A3B*, and *A3G*-related genes.

3. Results

1 Expression of APOBEC Family Members in PBMCs of COVID-19 Patients

Gene expression data in PBMCs of COVID-19 patients and healthy individuals were categorized into five groups: 50 ICU patients, 50 patients with moderate symptoms, 4 patients with mild symptoms, 43 asymptomatic individuals, and 5 healthy controls. The transcriptional levels of 8 APOBEC family members were extracted for differential mRNA level expression analysis, consisting of *A2*, *A3A*, *A3B*, *A3C*, *A3D*, *A3F*, *A3G* and *A3H*. It was found that mRNA expression of *A3A*, *A3B*, and *A3G* increased with disease severity, while other members did not show significant differences (Supplementary Fig. 1). In addition, mRNA expression level of *A3A* was significantly higher in PBMCs of the ICU patients and patients with moderate symptoms than in those of healthy controls. No significant difference was found between mildly ill or asymptomatic SARS-CoV-2-infected subjects and healthy individuals (Fig. 1A). mRNA expression of *A3B* was significantly higher in PBMCs of COVID-19 ICU patients and COVID-19 patients with moderate symptoms than in those of healthy controls (Fig. 1A). mRNA expression level of *A3B* in PBMCs of the mildly ill COVID-19 patients was higher than that of asymptomatic SARS-CoV-2-infected subjects. mRNA expression of *A3G* was significantly higher in PBMCs of COVID-19 patients with moderate symptoms than in those of ICU patients (Fig. 1A).

2 GO and KEGG Analysis of *A3A*, *A3B* and *A3G* Related Gene Expression Profiles

We conducted GO and KEGG analyses of gene functions and relevant signaling pathways of gene expression profiles related to *A3A*, *A3B*, and *A3G* in PBMCs of the patients with moderate symptoms and ICU patients, respectively. The GO analysis revealed that *A3A*, *A3B*, and *A3G* were enriched in gene functions related to virus response, defense response to virus, response to type I interferon (IFN–I), IFN-I signaling pathway, and cellular response to IFN-I (Fig. 1B). The KEGG analysis indicated that *A3A*, *A3B*, and *A3G* genes were jointly enriched in signaling pathways including Epstein−Barr virus infection, influenza A, hepatitis C, and measles (Fig. 1C).

3 Correlations of the Expression Levels of *A3A*, *A3B*, and *A3G* with the Proportion of Each Immune Cell Type in SARS-CoV-2-Infected Subjects with Different Disease Severity

The proportion of each immune cell type was analyzed in PBMCs of ICU patients with COVID-19 and COVID-19 patients with moderate symptoms (Supplementary Fig. 2A, n = 100), COVID-19 patients with mild symptoms (Supplementary Fig. 2B, n = 4), and asymptomatic SARS-CoV-2 carriers (Supplementary Fig. 2C, n = 43). Notably, the proportion of patients with 20 % or more neutrophils in PBMCs was higher in the ICU and moderately ill COVID-19 patients (77 %) than that in those with mild symptoms (75 %) and asymptomatic SARS-CoV-2 infected subjects (41.9 %). We then investigated the correlation between mRNA expression levels of *A3A*, *A3B*, and *A3G* and the proportion of each of the 17 immune cell types in PBMCs of the SARS-CoV-2 infected subjects with three levels of disease severity (Fig. 2). The correlation between mRNA expression level of *A3A* and the proportion of naive $CD4^+$ T cells, or resting memory $CD4^+$ T cells, increased with disease severity. The correlation between mRNA expression of *A3B* and the proportion of neutrophils, or resting memory $CD4^+$ T cells, and the correlation between mRNA expression of *A3G* and the proportion of resting memory $CD4^+$ T cells also increased with the severity of disease (Fig. 2).

4 Identification of Core Genes Related to Key APOBEC3 Proteins

We investigated the up-regulated and down-regulated DEGs in mRNA expression profiles from PBMCs of ICU COVID-19 patients and COVID-19 patients with moderate symptoms (Fig. 3A, Supplementary Fig. 3). In total, 40 genes commonly up-regulated and 2

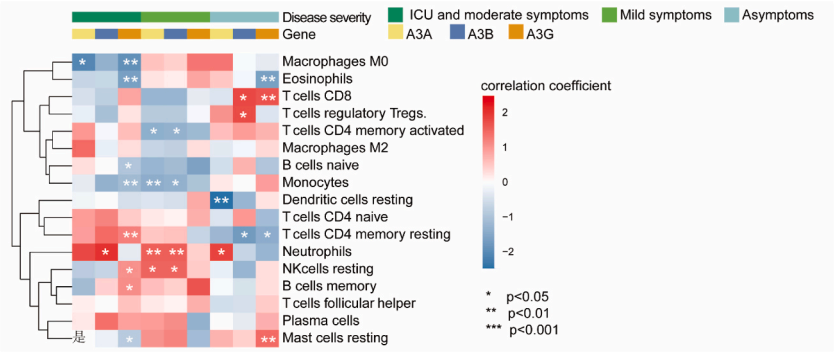

Fig. 2. Correlation of mRNA expression levels of *A3A*, *A3B*, and *A3G* with the proportion of each immune cell type in PBMCs of SARS-CoV-2 infected subjects with different disease severity. Coefficients of mRNA expression levels of *A3A*, *A3B*, and *A3G* with the proportion of each immune cell type with the severity of COVID-19 were evaluated using CIBERSORT algorithm. The red color represents positive correlation, and the blue color represents negative correlation.

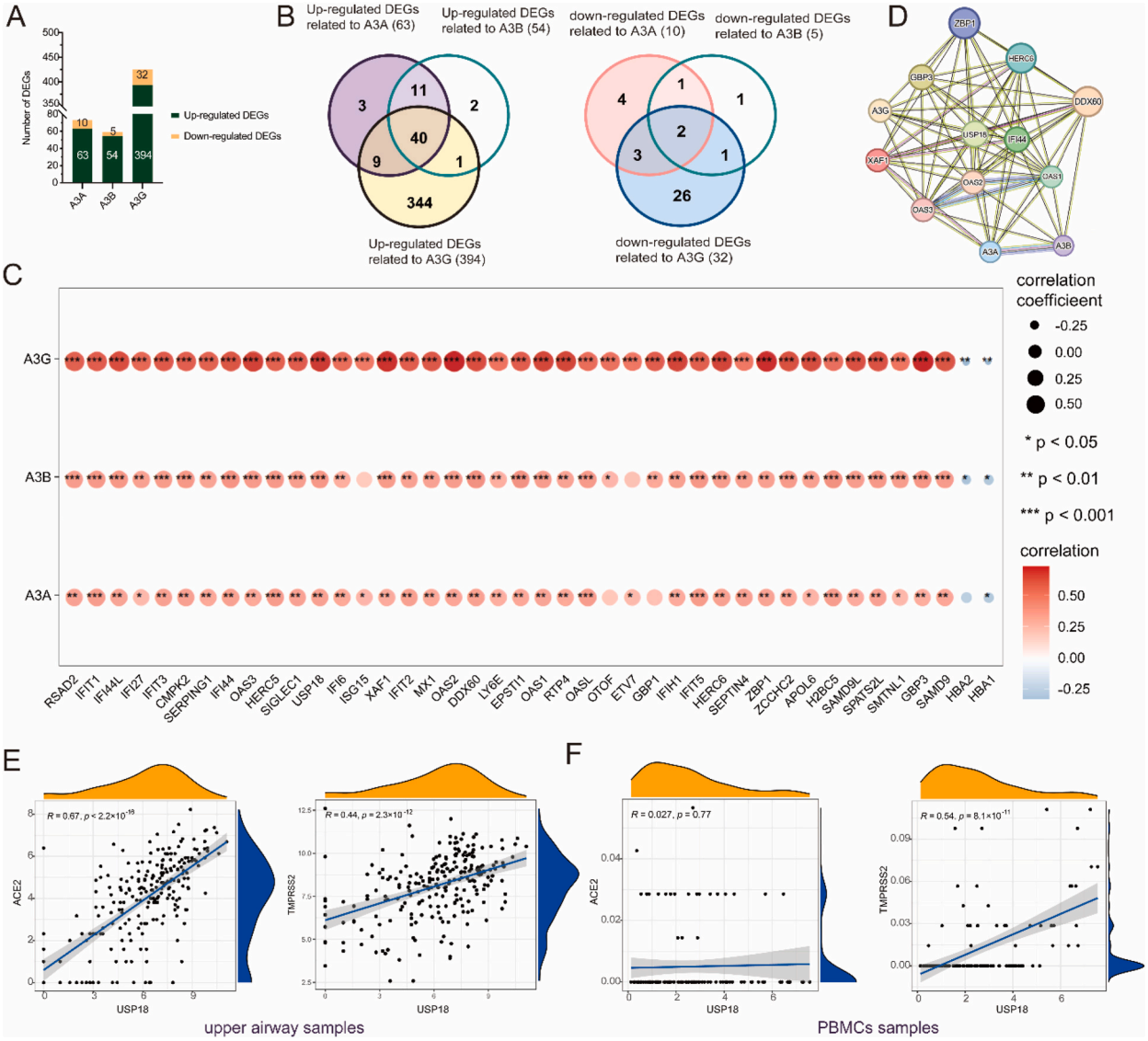

Fig. 3. Correlation of DEGs with *A3A*, *A3B*, and *A3G* gene expression in PBMCs and upper airways tissues of SARS-CoV-2-infected subjects and their core network (A) The DEGs were displayed in a bar plot. Dark green represents up-regulated DEGs and yellow represents down-regulated DEGs. (B) Venn diagrams about the overlapping DEGs were demonstrated. The left one represented up-regulated DEGs and the right one represented down-regulated DEGs. (C) The correlation of up-regulated and down-regulated genes was displayed in a bubble plot. Dots represent the correlation coefficient, while asterisks represent P-value. The red color indicated a positive correlation, while the blue color indicated a negative correlation. (D) The PPI network among A3A, A3B, and A3G proteins and the top 10 significantly upregulated proteins was constructed using the STRING database. (E) Correlation analyses between the gene transcription of *USP18* and *ACE2* (left) or *TMPRSS2* (right) in the tissue of upper airways from the GSE156063 dataset were displayed in scatter diagrams. (F) Correlation analyses between the gene transcription of *USP18* and *ACE2* (left) or *TMPRSS2* (right) in PBMCs from the GSE157103 dataset were displayed in scatter diagrams. (For interpretation of the references to color in this figure legend, the reader is referred to the Web version of this article.)

genes commonly down-regulated, compared with the medians of *A3A*, *A3B*, and *A3G* genes, were identified (Fig. 3B). Their correlation with key APOBEC3 proteins was constructed (Fig. 3C) and then ranked based on their correlation coefficients (Supplementary Table 2). Because of few literature on the associations of down-regulated genes with SARS-CoV-2, we selected top 10 up-regulated genes (*USP18, OAS2, GBP3, DDX60, ZBP1, XAF1, HERC6, IF144, OAS3* and *OAS1*) and then focused on the genes with the highest total correlation coefficients, namely *USP18* and *OAS2*. Notably, USP18 protein was located at the center of the PPI network (Fig. 3D). The network hub, USP18, had a high probability of engaging in essential biological functions [34]. Therefore, we chose the *USP18* gene for subsequent analysis. mRNA expression of *USP18* was strongly correlated with *ACE2* and *TMPRSS2* in the tissues of upper airways (Fig. 3E). However, *USP1*8 mRNA expression was not significantly correlated with the *ACE2* mRNA expression in PBMCs (Fig. 3F).

5 The Effects of Viral Infection on the Gene Expression of *A3A*, *A3B*, *A3G* and *USP18*

We examined the effect of viral infection on the expression of *A3A*, *A3B*, and *A3G* gene in 239T-ACE2, HeLa-ACE2, H1650, and Huh7 cell lines, comparing their mRNA levels between control and virus-infected cells. It was found that mRNA expression levels of *A3B* and *USP18,* rather than *A3A* and *A3G*, were significantly up-regulated by the infection with Omicron BA.4/5 S protein pseudovirus (Fig. 4A and B). We also observed an increased level of A3B protein in Huh7 and H1650 cells infected with the pseudovirus (Fig. 4C). H1650 cells were transfected with si-USP18-1, si-USP18-2, and si-USP18-3 siRNA reagents. si-USP18-1 was proven to be the most effective in silencing the expression of *USP18* (Fig. 4D). mRNA expression of *A3B* was significantly down-regulated in H1650 cells with *USP18* gene knocked down no matter if the pseudovirus was added, indicating a positive correlation between *USP18* and *A3B* gene (Fig. 4E). Subsequently, luciferase reporter assay was performed to investigate the effect of *A3B* gene on SARS-CoV-2 infection, as the luciferase activity can reflect the ability of virus binding to cell surface. We infected Huh7 cells overexpressing A3B protein and control cells with wild-type SARS-CoV-2 S protein pseudovirus and Omicron BA.4/5 S protein pseudovirus, respectively. It was found that relative luciferase units (RLU) values in Huh7 cells overexpressing A3B protein were significantly higher than those in the control group, suggesting that A3B overexpression facilitates SARS-CoV-2 infection (Fig. 4F).

6 Effects of APOBEC3-Related C > U Mutation Sites on the Infectivity and Immune Escape Capacity of SARS-CoV-2

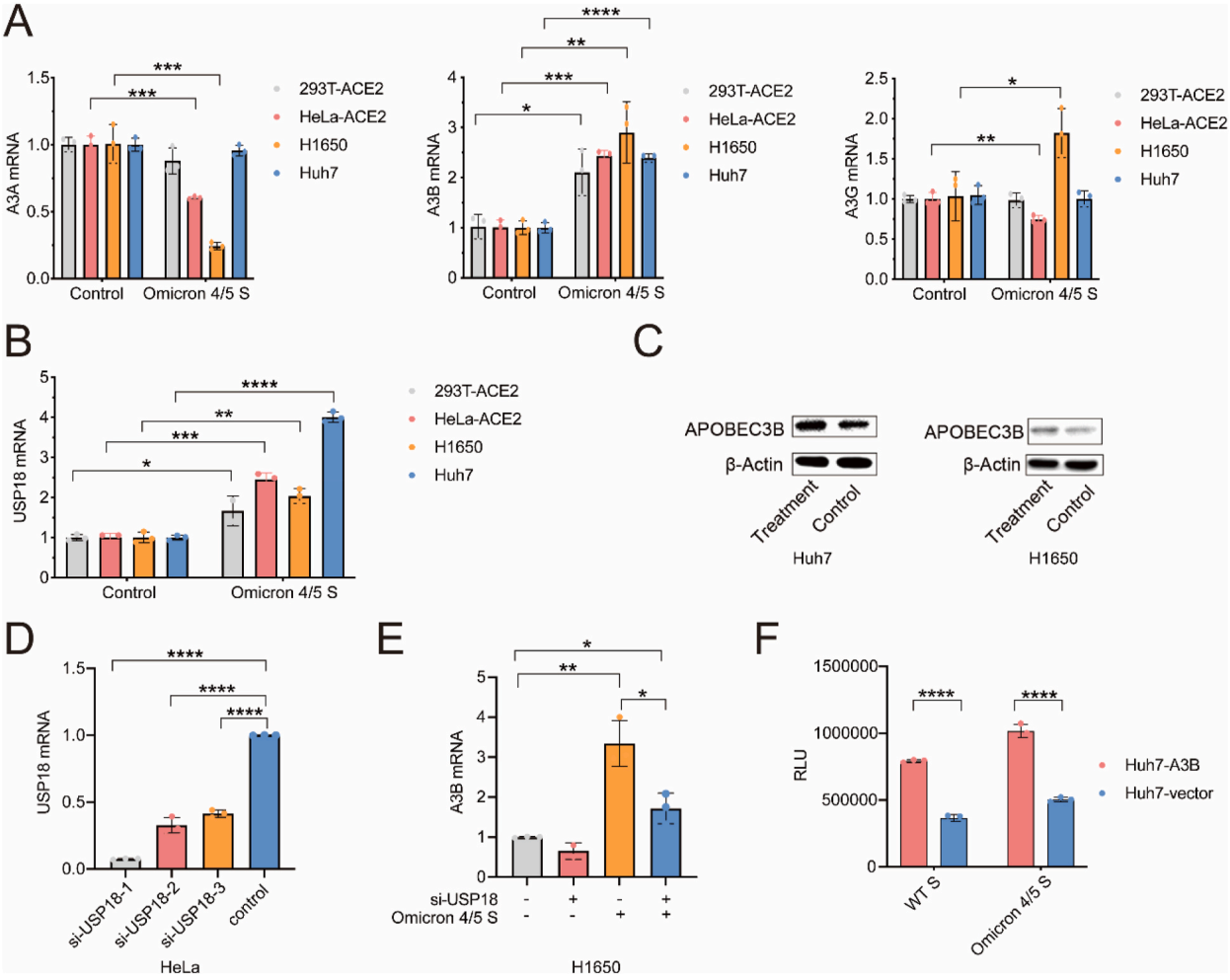

Fig. 4. The interaction of *A3B* and *USP18* gene expression with the infection of pseudovirus carrying S protein from wildtype SARS-CoV-2 and Omicron BA.4/5 (A) The effect of Omicron BA.4/5 S protein pseudovirus infection on mRNA expression levels of *A3A* (left), *A3B* (middle), and *A3G* (right) in 293T-ACE2, H1650, HeLa-ACE2, and Huh7 cells before and after infection with Omicron BA.4/5 S protein pseudovirus displayed in histograms. (B) The effect of Omicron BA.4/5 S protein pseudovirus infection on mRNA expression levels of *USP18* in 293T-ACE2, H1650, HeLa-ACE2, and Huh7 cells. (C) The level of A3B protein in Huh7 (left) and H1650 (right) cells before and after Omicron BA.4/5 S protein pseudovirus infection. (D) The effect of three *USP18* siRNAs on mRNA expression levels of *USP18* in HeLa cells. (E) The effect of silencing *USP18* on mRNA expression of *A3B* in H1650 upon Omicron BA.4/5 S protein pseudovirus infection. (F) The infectivity of wild-type SARS-CoV-2 S pseudovirus or Omicron BA.4/5 S protein pseudovirus in Huh7 cells-overexpressing A3B protein.

The SARS-CoV-2 sequences randomly selected from the database were divided into five groups based on the isolation time: 2019.12–2020.03, 2020.03–2020.06, 2020.06–2020.09, 2020.09–2020.12, and 2020.12–2021.05. The frequency of missense C > U mutation increased from December 2019 to May 2021, while that of synonymous C > U mutation decreased since March–June 2020 (Supplementary Fig. 4A). The number of C > U mutations ranked second among all single nucleotide substitution mutations (Supplementary Fig. 4B). Additionally, sequences with C > U mutations were continuously evolving within overlapped branches, implying their aggregation and evolution (Supplementary Fig. 4C).

We introduced a single-point mutation into the wild-type S protein with D614G which is present in over 90 % of SARS-CoV-2 isolates [35]. According to APOBEC3-targeted TCW motif, we designed 13 C > U mutations, namely, S325F, S366F, S371F, S373L, S375F, S383F, S399L, S438F, S443F, S459F, S469F, S494L and S514F in the RBD region, created a single-point mutation on the S gene, produced the pseudovirus, and infected the cell lines, respectively. The infectivity of most pseudoviruses carrying the mutated S gene was significantly decreased, compared with the reference sequence (Fig. 5A). Interestingly, the S gene with S371F, S373L, or S375F mutation displayed a significant increase in viral immune escape capacity (Fig. 5B). Furthermore, all of these mutations altered hydrogen bonds of affected amino acids in the S protein. Prior to mutation, the S371 site exhibited hydrogen bonding interactions with the S373 site and the L368 site. However, a hydrogen bond with the S373 site was abolished, and only a hydrogen bond with the L368 site remained following the mutation from S371 to F371. The S373 site formed a hydrogen bond with the S371 site before mutation. However, after mutating to L373, hydrogen bond interaction was abolished. The S375 formed two hydrogen bonds with A435 before mutation, but after switched to F375, only one hydrogen bond with A435 remained (Fig. 5C). The SARS-CoV-2 genomes with S371F and S375F mutations were notably detected after October 2021 (Fig. 5D). Consequently, three point mutations were selected from an initial pool of 13 APOBEC3-related mutations.

4. Discussion

During the COVID-19 pandemic, SARS-CoV-2 evolves consecutively [36,37], with C > U mutations being a major contributor [38]. APOBEC3-induced C > U mutation, an important source of viral mutations in the inflammatory microenvironment, has not been extensively investigated in viral evolution. Data in this study indicate that *A3B* gene is highly expressed in HEK293T-ACE2, H1650, HeLa-ACE2, and Huh7 cell lines infected with SARS-CoV-2 pseudovirus (Fig. 4A) and positively correlates with *USP18* gene (Fig. 4B). Meanwhile, *USP18* gene is positively related to the expression of *TMPRSS2* gene which facilitates viral entry [39]. A3B protein is upregulated by inflammatory cytokines such as IL-6 [20] and promotes *TMPRSS2* gene expression using *USP18* as a bridge to affect viral infection. On the other hand, higher *A3B* expression promotes SARS-CoV-2 to mutate and evolve, contributing to the increased

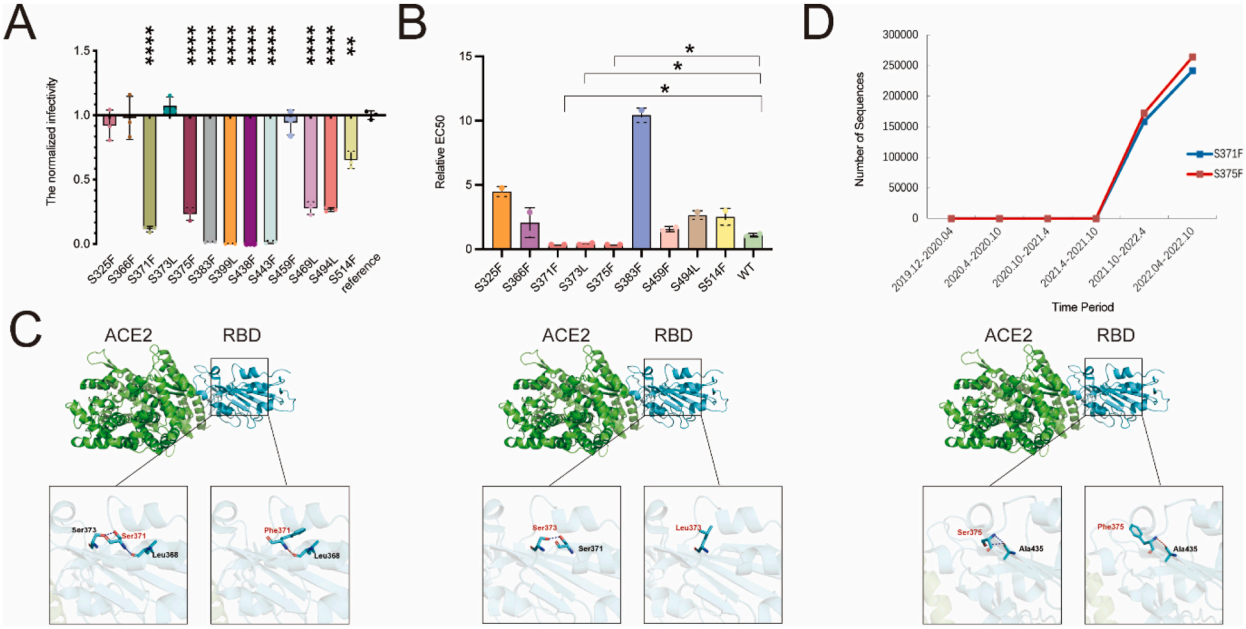

Fig. 5. Effect of C > U mutations on the infectivity and immune evasion capacity of SARS-CoV-2 (A) Changes in the infectivity of pseudovirus with different C > U mutations. The RLU values were normalized by setting the infectivity of the reference to 1. (B) Immune escape ability of pseudovirus with different C > U mutations was shown in bar graphs. The EC_{50} values were normalized by setting the reference to 1. (C) The effects of S371F (left), S373L (middle), and S375F (right) on alteration in the conformation of the S protein's RBD region of SARS-CoV-2 was visualized by PyMOL. The images illustrate the crystal structure of SARS-CoV-2 spike RBD bound with ACE2. In the boxes below, the left image represents the conformation of the RBD of spike protein before the mutation, while the right image represents conformation of the RBD of the spike protein after mutation. (D) The replication of SARS-CoV-2 containing S371F and S375F increased rapidly and became epidemic after October 2021. The vertical axis represents the number of sequences, while the horizontal axis represents the time period.

infectivity. Our study also presents some new evidence of positive association between each of the three C > U mutations (S371F, S373L, and S375F) and viral immune escape (Fig. 5B).

A3B enzyme is a cytosine deaminase that catalyzes cytosine to uracil in RNA or single-stranded DNA, leading to hyper-mutation [20]. Although A3B is localized in the nucleus, it can be translocated to the cytoplasm after being infected by virus. Certain residues within A3B can predispose it to cytoplasmic localization upon HIV-1 infection [40]. Additionally, intracellular double-stranded RNA sensors facilitate the recruitment of A3B from the nucleus to stress granules within the cytoplasm by host proteins after detecting viral RNA [41]. In the present study, we revealed that *A3B* gene was positively related to neutrophils which contributed to disease severity. Levels of inflammation are increased in COVID-19 patients and A3B protein can be activated by IL-6 [30], thus enhancing *A3B* gene expression in the inflammatory microenvironment. APOBEC3 proteins also bind to the coronaviral nucleoprotein, affecting viral replication [42]. A3B enzyme has deaminase activity, contributing partially to viral mutagenesis; it also interacts with viral proteins, potentially influencing viral infection [41]. In addition, A3A has also been implicated in driving mutations in SARS-CoV-2 [24], but a limitation of this previous study is the absence of experimental data to support this claim.

In the present study, we found that *A3B* gene was positively associated with *USP18 gene*, while *USP18* was positively related with *ACE2* and *TMPRSS2* gene in the tissue of upper airways, indicating an active role of *A3B* in viral infection. USP18 protein is an IFN-stimulated gene product and a negative regulator of IFN-I signaling [43]. USP18 is highly expressed in liver, lung and kidney. The ISG15/USP18 pathway is vital for innate immune response to viral infections [44]. *USP18* gene is positively correlated with the expression of *TMPRSS2*, *CTSB*, and *CTSL* in blood leukocytes samples [45], implying that USP18 may be positively linked to SARS-CoV-2 infection. However, the impact of silencing A3B on viral infection still needs to be investigated. We observed in our experiments that C > U mutations decreased the infectivity of the pseudovirus, possibly due to the initial antiviral efficacy of APOBEC3 (reviewed in) [42]. APOBEC3 may facilitate SARS-CoV-2 infection, and significantly promote SARS-CoV-2 replication in later viral evolution [25], reflecting a dynamic interplay between viral mutations and the host's immune selection [46].

Furthermore, we identified three noteworthy mutation sites: S373L, S371F [47], and S375F [48], two of which appeared in Omicron BA.1 and BA.2 variants [48]. These mutation sites were specifically chosen based on the APOBEC3-targeted TCW motif patterns. It is contradictory that the S pseudoviruses with S371F, S373L, or S375F exhibit an increased immune escape ability but have lower infectivity. The S371F and S375F mutations promote interactions among "downward RBDs", leading to the closure of the S protein conformation and reduction of the viral infectivity [49,50], but also increase the immune evasion ability of the virus [51]. The S375F mutation is a key site accounting for the emergence of Omicron [52]. Residues F375 and H505 form π-π interactions in the Omicron S protein trimer, which significantly affects the S protein cleavage ability and fusion activity [48]. All these evidences suggest that immune evasion may be the primary driving force behind Omicron's evolution. More researches are needed to clarify the factors responsible for the further evolution of this virus.

Our study yielded several key findings. First, APOBEC3s especially A3A and A3B were upregulated in severe SARS-CoV-2 infection. Second, USP18 facilitated the expression of SARS-CoV-2 receptors in upper airway epithelial, increased the expression of A3B, while A3B facilitated the infection of SARS-CoV-2. Third, APOBEC3-related C > U mutations (S371F, S373L, and S375F) decreased the infectivity at early stage and confer with immune escape capacity, thus facilitating SARS-CoV-2 evolution. However, our study has limitations. First, some key findings were obtained from public datasets, which needs independent cohort of SARS-CoV-2 patients to validate. Second, pseudoviruses were used to test the biological effects, due to the limitation of our laboratory conditions, which might cause bias especially in examining the capacity of infectivity.

In summary, APOBEC3 family members especially A3A and A3B are significantly upregulated in severe patients with SARS-CoV-2 infection and related to viral and IFN-I signaling pathways. A3B is correlated to neutrophil and increases with increasing disease severity. USP18, an APOBEC3-related network hub, is positively correlated to the expression of SARS-CoV-2 receptors in upper airway epithelial, and promotes A3B expression, while A3B facilitates the infection of SARS-CoV-2. APOBEC3-related C > U mutations in the RBD region decrease the infectivity at early stage and confer with immune escape capacity, thus facilitating SARS-CoV-2 evolution. A3B and USP18 might be key therapeutic targets for interfering with SARS-CoV-2 evolution.

Funding

This research was funded by the National Natural Science Foundation of China (82041022); Shanghai Commission of Science and Technology (20JC1410200; 20431900404).

Informed consent statements

Not applicable.

Data availability statements

All genome sequences involved in this study were downloaded from the GISAID (https://www.gisaid.org/) and the expression profile was downloaded from the GEO (https://www.ncbi.nlm.nih.gov/geo/GEO) database, including dataset GSE157103, GSE162562, and GSE156063. The initial viral sequence (Wuhan-Hu-1 strain, GenBank: MN908947.3) was used as the reference sequence.

CRediT authorship contribution statement

Jiaying Shen: Writing – review & editing, Writing – original draft, Visualization, Project administration, Conceptualization. **Xinxin Xu:** Visualization, Software, Formal analysis, Data curation. **Junyan Fan:** Validation, Methodology. **Hongsen Chen:** Writing – review & editing, Writing – original draft, Project administration. **Yue Zhao:** Validation, Methodology. **Weijin Huang:** Writing – review & editing, Validation. **Wenbin Liu:** Writing – review & editing, Validation. **Zihan Zhang:** Writing – review & editing. **Qianqian Cui:** Validation, Methodology. **Qianqian Li:** Methodology, Investigation. **Zheyun Niu:** Writing – review & editing, Visualization. **Dongming Jiang:** Writing – review & editing. **Guangwen Cao:** Writing – review & editing, Supervision, Project administration.

Declaration of competing interest

The authors declare that they have no known competing financial interests or personal relationships that could have appeared to influence the work reported in this paper.

Appendix A. Supplementary data

Supplementary data to this article can be found online at https://doi.org/10.1016/j.heliyon.2024.e32139.

References

[1] J. Majumder, T. Minko, Recent developments on therapeutic and diagnostic approaches for COVID-19, AAPS J. 23 (1) (2021) 14, https://doi.org/10.1208/s12248-020-00532-2.
[2] K. Shehzad, L. Xiaoxing, F. Bilgili, E. Koçak, COVID-19 and spillover effect of global economic crisis on the United States' financial stability, Front. Psychol. 12 (2021) 632175, https://doi.org/10.3389/fpsyg.2021.632175.
[3] H. Akkiz, Implications of the novel mutations in the SARS-CoV-2 genome for transmission, disease severity, and the vaccine development, Front. Med. 8 (2021) 636532, https://doi.org/10.3389/fmed.2021.636532.
[4] B. Hu, H. Guo, P. Zhou, Z.L. Shi, Characteristics of SARS-CoV-2 and COVID-19, Nat. Rev. Microbiol. 19 (3) (2021) 141–154, https://doi.org/10.1038/s41579-020-00459-7.
[5] F. Kabinger, C. Stiller, J. Schmitzová, C. Dienemann, G. Kokic, H.S. Hillen, et al., Mechanism of molnupiravir-induced SARS-CoV-2 mutagenesis, Nat. Struct. Mol. Biol. 28 (9) (2021) 740–746, https://doi.org/10.1038/s41594-021-00651-0.
[6] J. Ou, W. Lan, X. Wu, T. Zhao, B. Duan, P. Yang, et al., Tracking SARS-CoV-2 Omicron diverse spike gene mutations identifies multiple inter-variant recombination events, Signal Transduct. Targeted Ther. 7 (1) (2022) 138, https://doi.org/10.1038/s41392-022-00992-2.
[7] D. Chauhan, N. Chakravarty, A.V. Jeyachandran, A. Jayakarunakaran, S. Sinha, R. Mishra, et al., In silico genome analysis reveals the evolution and potential impact of SARS-CoV-2 Omicron structural changes on host immune evasion and antiviral therapeutics, Viruses 14 (11) (2022), https://doi.org/10.3390/v14112461.
[8] J. Chen, R. Wang, N.B. Gilby, G.W. Wei, Omicron variant (B.1.1.529): infectivity, vaccine breakthrough, and antibody resistance, J. Chem. Inf. Model. 62 (2) (2022) 412–422, https://doi.org/10.1021/acs.jcim.1c01451.
[9] S. Iketani, L. Liu, Y. Guo, L. Liu, J.F. Chan, Y. Huang, et al., Antibody evasion properties of SARS-CoV-2 Omicron sublineages, Nature 604 (7906) (2022) 553–556, https://doi.org/10.1038/s41586-022-04594-4.
[10] Y. Cao, F. Jian, J. Wang, Y. Yu, W. Song, A. Yisimayi, et al., Imprinted SARS-CoV-2 humoral immunity induces convergent Omicron RBD evolution, Nature 614 (7948) (2023) 521–529, https://doi.org/10.1038/s41586-022-05644-7.
[11] C.C. Bradley, C. Wang, A.J.E. Gordon, A.X. Wen, P.N. Luna, M.B. Cooke, et al., Targeted accurate RNA consensus sequencing (tARC-seq) reveals mechanisms of replication error affecting SARS-CoV-2 divergence, Nature microbiology (2024 Apr 22), https://doi.org/10.1038/s41564-024-01655-4.
[12] K.D. Lamb, M.M. Luka, M. Saathoff, R.J. Orton, M.V.T. Phan, M. Cotten, et al., Mutational signature dynamics indicate SARS-CoV-2's evolutionary capacity is driven by host antiviral molecules, PLoS Comput. Biol. 20 (1) (2024) e1011795, https://doi.org/10.1371/journal.pcbi.1011795.
[13] A. Graudenzi, D. Maspero, F. Angaroni, R. Piazza, D. Ramazzotti, Mutational signatures and heterogeneous host response revealed via large-scale characterization of SARS-CoV-2 genomic diversity, iScience 24 (2) (2021) 102116, https://doi.org/10.1016/j.isci.2021.102116.
[14] S. Revathidevi, A.K. Murugan, H. Nakaoka, I. Inoue, A.K. Munirajan, APOBEC: a molecular driver in cervical cancer pathogenesis, Cancer Lett. 496 (2021) 104–116, https://doi.org/10.1016/j.canlet.2020.10.004.
[15] M. Bonvin, F. Achermann, I. Greeve, D. Stroka, A. Keogh, D. Inderbitzin, et al., Interferon-inducible expression of APOBEC3 editing enzymes in human hepatocytes and inhibition of hepatitis B virus replication, Hepatology 43 (6) (2006) 1364–1374, https://doi.org/10.1002/hep.21187.
[16] S. Venkatesan, R. Rosenthal, N. Kanu, N. McGranahan, J. Bartek, S.A. Quezada, et al., Perspective: APOBEC mutagenesis in drug resistance and immune escape in HIV and cancer evolution, Ann. Oncol. 29 (3) (2018) 563–572, https://doi.org/10.1093/annonc/mdy003.
[17] V. Rayon-Estrada, D. Harjanto, C.E. Hamilton, Y.A. Berchiche, E.C. Gantman, T.P. Sakmar, et al., Epitranscriptomic profiling across cell types reveals associations between APOBEC1-mediated RNA editing, gene expression outcomes, and cellular function, Proc. Natl. Acad. Sci. U.S.A. 114 (50) (2017) 13296–13301, https://doi.org/10.1073/pnas.1714227114.
[18] S. Sharma, S.K. Patnaik, R.T. Taggart, E.D. Kannisto, S.M. Enriquez, P. Gollnick, et al., APOBEC3A cytidine deaminase induces RNA editing in monocytes and macrophages, Nat. Commun. 6 (2015) 6881, https://doi.org/10.1038/ncomms7881.
[19] G. Tang, B. Xie, X. Hong, H. Qin, J. Wang, H. Huang, et al., Creating RNA specific C-to-U editase from APOBEC3A by separation of its activities on DNA and RNA substrates, ACS Synth. Biol. 10 (5) (2021) 1106–1115, https://doi.org/10.1021/acssynbio.0c00627.
[20] A. Alonso de la Vega, N.A. Temiz, R. Tasakis, K. Somogyi, L. Salgueiro, E. Zimmer, et al., Acute expression of human APOBEC3B in mice results in RNA editing and lethality, Genome Biol. 24 (1) (2023) 267, https://doi.org/10.1186/s13059-023-03115-4.
[21] J. Li, G. Fan, M. Sakari, T. Tsukahara, Improvement of C-to-U RNA editing using an artificial MS2-APOBEC system, Biotechnol. J. 19 (1) (2024) e2300321, https://doi.org/10.1002/biot.202300321.
[22] A. Meshcheryakova, P. Pietschmann, P. Zimmermann, I.B. Rogozin, D. Mechtcheriakova, AID and APOBECs as multifaceted intrinsic virus-restricting factors: emerging concepts in the light of COVID-19, Front. Immunol. 12 (2021) 690416, https://doi.org/10.3389/fimmu.2021.690416.
[23] P. Simmonds, Rampant C→U hypermutation in the genomes of SARS-CoV-2 and other coronaviruses: causes and consequences for their short- and long-term evolutionary trajectories, mSphere 5 (3) (2020), https://doi.org/10.1128/mSphere.00408-20.

[24] Y. Nakata, H. Ode, M. Kubota, T. Kasahara, K. Matsuoka, A. Sugimoto, et al., Cellular APOBEC3A deaminase drives mutations in the SARS-CoV-2 genome, Nucleic Acids Res. 51 (2) (2023) 783–795, https://doi.org/10.1093/nar/gkac1238.
[25] K. Kim, P. Calabrese, S. Wang, C. Qin, Y. Rao, P. Feng, et al., The roles of APOBEC-mediated RNA editing in SARS-CoV-2 mutations, replication and fitness, Sci. Rep. 12 (1) (2022) 14972, https://doi.org/10.1038/s41598-022-19067-x.
[26] A.M. Newman, C.L. Liu, M.R. Green, A.J. Gentles, W. Feng, Y. Xu, et al., Robust enumeration of cell subsets from tissue expression profiles, Nat. Methods 12 (5) (2015) 453–457, https://doi.org/10.1038/nmeth.3337.
[27] D. Szklarczyk, R. Kirsch, M. Koutrouli, K. Nastou, F. Mehryary, R. Hachilif, et al., The STRING database in 2023: protein-protein association networks and functional enrichment analyses for any sequenced genome of interest, Nucleic Acids Res. 51 (D1) (2023) D638, https://doi.org/10.1093/nar/gkac1000, d46.
[28] Y.Q. Zhou, K. Wang, X.Y. Wang, H.Y. Cui, Y. Zhao, P. Zhu, et al., SARS-CoV-2 pseudovirus enters the host cells through spike protein-CD147 in an Arf6-dependent manner, Emerg. Microb. Infect. 11 (1) (2022) 1135–1144, https://doi.org/10.1080/22221751.2022.2059403.
[29] W. Zhou, C. Xu, P. Wang, A.A. Anashkina, Q. Jiang, Impact of mutations in SARS-COV-2 spike on viral infectivity and antigenicity, Briefings Bioinf. 23 (1) (2022), https://doi.org/10.1093/bib/bbab375.
[30] W. Liu, J. Wu, F. Yang, L. Ma, C. Ni, X. Hou, et al., Genetic polymorphisms predisposing the interleukin 6-induced APOBEC3B-ung imbalance increase HCC risk via promoting the generation of APOBEC-signature HBV mutations, Clin. Cancer Res. 25 (18) (2019) 5525–5536, https://doi.org/10.1158/1078-0432.Ccr-18-3083.
[31] Q. Li, J. Wu, J. Nie, L. Zhang, H. Hao, S. Liu, et al., The impact of mutations in SARS-CoV-2 spike on viral infectivity and antigenicity, Cell 182 (5) (2020) 1284, https://doi.org/10.1016/j.cell.2020.07.012, 94.e9.
[32] J. Nie, Q. Li, J. Wu, C. Zhao, H. Hao, H. Liu, et al., Establishment and validation of a pseudovirus neutralization assay for SARS-CoV-2, Emerg. Microb. Infect. 9 (1) (2020) 680–686, https://doi.org/10.1080/22221751.2020.1743767.
[33] P.H. Yang, Y.B. Ding, Z. Xu, R. Pu, P. Li, J. Yan, et al., Increased circulating level of interleukin-6 and CD8(+) T cell exhaustion are associated with progression of COVID-19, Infectious diseases of poverty 9 (1) (2020) 161, https://doi.org/10.1186/s40249-020-00780-6.
[34] X. Tan, Y. Zhai, W. Chang, J. Hou, S. He, L. Lin, et al., Global analysis of metastasis-associated gene expression in primary cultures from clinical specimens of clear-cell renal-cell carcinoma, Int. J. Cancer 123 (5) (2008) 1080–1088, https://doi.org/10.1002/ijc.23637.
[35] B. Korber, W.M. Fischer, S. Gnanakaran, H. Yoon, J. Theiler, W. Abfalterer, et al., Tracking changes in SARS-CoV-2 spike: evidence that D614G increases infectivity of the COVID-19 virus, Cell 182 (4) (2020) 812, https://doi.org/10.1016/j.cell.2020.06.043, 27.e19.
[36] V. Thakur, S. Bhola, P. Thakur, S.K.S. Patel, S. Kulshrestha, R.K. Ratho, et al., Waves and variants of SARS-CoV-2: understanding the causes and effect of the COVID-19 catastrophe, Infection 50 (2) (2022) 309–325, https://doi.org/10.1007/s15010-021-01734-2.
[37] M. Ghafari, M. Hall, T. Golubchik, D. Ayoubkhani, T. House, G. MacIntyre-Cockett, et al., Prevalence of persistent SARS-CoV-2 in a large community surveillance study, Nature (2024), https://doi.org/10.1038/s41586-024-07029-4.
[38] Y. Li, F. Hou, M. Zhou, X. Yang, B. Yin, W. Jiang, et al., C-to-U RNA deamination is the driving force accelerating SARS-CoV-2 evolution, Life Sci. Alliance 6 (1) (2023), https://doi.org/10.26508/lsa.202201688.
[39] W. Liu, Y. Zhao, J. Fan, J. Shen, H. Tang, W. Tang, et al., Smoke and spike: benzo[a]pyrene enhances SARS-CoV-2 infection by boosting nr4a2-induced ACE2 and TMPRSS2 expression, Adv. Sci. 10 (26) (2023) e2300834, https://doi.org/10.1002/advs.202300834.
[40] M. Marin, S. Golem, K.M. Rose, S.L. Kozak, D. Kabat, Human immunodeficiency virus type 1 Vif functionally interacts with diverse APOBEC3 cytidine deaminases and moves with them between cytoplasmic sites of mRNA metabolism, J. Virol. 82 (2) (2008) 987–998, https://doi.org/10.1128/jvi.01078-07.
[41] L. Manjunath, S. Oh, P. Ortega, A. Bouin, E. Bournique, A. Sanchez, et al., APOBEC3B drives PKR-mediated translation shutdown and protects stress granules in response to viral infection, Nat. Commun. 14 (1) (2023) 820, https://doi.org/10.1038/s41467-023-36445-9.
[42] A. Milewska, E. Kindler, P. Vkovski, S. Zeglen, M. Ochman, V. Thiel, et al., APOBEC3-mediated restriction of RNA virus replication, Sci. Rep. 8 (1) (2018) 5960, https://doi.org/10.1038/s41598-018-24448-2.
[43] M. Martin-Fernandez, S. Buta, T. Le Voyer, Z. Li, L.T. Dynesen, F. Vuillier, et al., A partial form of inherited human USP18 deficiency underlies infection and inflammation, J. Exp. Med. 219 (4) (2022), https://doi.org/10.1084/jem.20211273.
[44] L. Ketscher, R. Hannß, D.J. Morales, A. Basters, S. Guerra, T. Goldmann, et al., Selective inactivation of USP18 isopeptidase activity in vivo enhances ISG15 conjugation and viral resistance, Proc. Natl. Acad. Sci. U.S.A. 112 (5) (2015) 1577–1582, https://doi.org/10.1073/pnas.1412881112.
[45] X. Gao, Y. Liu, S. Zou, P. Liu, J. Zhao, C. Yang, et al., Genome-wide screening of SARS-CoV-2 infection-related genes based on the blood leukocytes sequencing data set of patients with COVID-19, J. Med. Virol. 93 (9) (2021) 5544–5554, https://doi.org/10.1002/jmv.27093.
[46] S.L. Pond, B. Murrell, A.F. Poon, Evolution of viral genomes: interplay between selection, recombination, and other forces, Methods Mol. Biol. 856 (2012) 239–272, https://doi.org/10.1007/978-1-61779-585-510.
[47] R. Nutalai, D. Zhou, A. Tuekprakhon, H.M. Ginn, P. Supasa, C. Liu, et al., Potent cross-reactive antibodies following Omicron breakthrough in vaccinees, Cell 185 (12) (2022) 2116, https://doi.org/10.1016/j.cell.2022.05.014, 31.e18.
[48] I. Kimura, D. Yamasoba, H. Nasser, J. Zahradnik, Y. Kosugi, J. Wu, et al., The SARS-CoV-2 spike S375F mutation characterizes the Omicron BA.1 variant, iScience 25 (12) (2022) 105720, https://doi.org/10.1016/j.isci.2022.105720.
[49] S.M. Gobeil, R. Henderson, V. Stalls, K. Janowska, X. Huang, A. May, et al., Structural diversity of the SARS-CoV-2 Omicron spike, Mol. Cell 82 (11) (2022) 2050, https://doi.org/10.1016/j.molcel.2022.03.028, 68.e6.
[50] C. Pastorio, F. Zech, S. Noettger, C. Jung, T. Jacob, T. Sanderson, et al., Determinants of Spike infectivity, processing, and neutralization in SARS-CoV-2 Omicron subvariants BA.1 and BA.2, Cell Host Microbe 30 (9) (2022) 1255, https://doi.org/10.1016/j.chom.2022.07.006, 68.e5.
[51] Z. Zhao, J. Zhou, M. Tian, M. Huang, S. Liu, Y. Xie, et al., Omicron SARS-CoV-2 mutations stabilize spike up-RBD conformation and lead to a non-RBM-binding monoclonal antibody escape, Nat. Commun. 13 (1) (2022) 4958, https://doi.org/10.1038/s41467-022-32665-7.
[52] K.A. Huang, X. Chen, A. Mohapatra, H.T.V. Nguyen, L. Schimanski, T.K. Tan, et al., Structural basis for a conserved neutralization epitope on the receptor-binding domain of SARS-CoV-2, Nat. Commun. 14 (1) (2023) 311, https://doi.org/10.1038/s41467-023-35949-8.